Polarization Transfer

International Edition: DOI: 10.1002/anie.201804185
German Edition: DOI: 10.1002/ange.201804185

More Than 12 % Polarization and 20 Minute Lifetime of ^{15}N in a Choline Derivative Utilizing Parahydrogen and a Rhodium Nanocatalyst in Water

Jeffrey McCormick, Sergey Korchak, Salvatore Mamone, Yavuz N. Ertas, Zhiyu Liu, Luke Verlinsky, Shawn Wagner, Stefan Glöggler, and Louis-S. Bouchard**

Abstract: *Hyperpolarization techniques are key to extending the capabilities of MRI for the investigation of structural, functional and metabolic processes in vivo. Recent heterogeneous catalyst development has produced high polarization in water using parahydrogen with biologically relevant contrast agents. A heterogeneous ligand-stabilized Rh catalyst is introduced that is capable of achieving ^{15}N polarization of 12.2 ± 2.7 % by hydrogenation of neurine into a choline derivative. This is the highest ^{15}N polarization of any parahydrogen method in water to date. Notably, this was performed using a deuterated quaternary amine with an exceptionally long spin-lattice relaxation time (T_1) of 21.0 ± 0.4 min. These results open the door to the possibility of ^{15}N in vivo imaging using nontoxic similar model systems because of the biocompatibility of the production media and the stability of the heterogeneous catalyst using parahydrogen-induced polarization (PHIP) as the hyperpolarization method.*

The inherently low sensitivity of magnetic resonance methods limits the scope of chemical and biological investigations in clinical contexts. This has motivated recent advancements in hyperpolarization techniques capable of generating several orders of magnitude signal enhancements with contrast agents such as metabolites. Dissolution dynamic nuclear polarization (d-DNP) can generate large polarizations on injectable contrast agents and has shown great promise in medical application,[1–4] even though DNP requires high capital equipment investment and requires several hours to produce a polarized sample prohibiting concepts such as continuous multiple infusions.[5] An alternative approach of hyperpolarization uses the singlet spin state isomer of hydrogen known as parahydrogen (para-H_2) to generate polarization by PHIP[6–8] and signal amplification by reversible exchange (SABRE).[9] These techniques are significantly more cost-effective as 100 % enriched para-H_2 can be easily generated by flowing H_2 gas over a catalyst at low temperatures and stored at room temperature. Additionally, the equipment has a lower base cost since only low magnetic fields are required eliminating the high acquisition cost of a superconducting magnet and maintenance.

The implementation of solution-state PHIP techniques which employs effective homogeneous catalysts in organic solvents and water pose concerns over the biotoxicity of the hyperpolarized product mixtures[10] and has motivated heterogeneous alternatives capable of high aqueous polarization. Although high ^{13}C polarizations (> 3 %) have recently been shown by labile transfer of cleavable [1-^{13}C]pyruvate derivatives into pure water using a homogeneous catalyst,[11] metal degradation was observed along with concerns of chemical stability in the presence of unprotected nitrogen groups, necessitating further method optimization. Excellent advances have been made with efficient ^{15}N polarization using the PHIP variants SABRE and SABRE-SHEATH; however, these methods have thus far been used to investigate compounds with subclinical ^{15}N polarizations,[12] optimization in organic solvents,[13,14] and limited development of heterogeneous catalysts.[15,16] While PHIP has been investigated in vivo,[17–21] clinical applications require the production of the non-toxic and preferably pure sterile product; a heterogeneous catalyst can be removed from the mixture after polarization enhancement creating a pure aqueous solution of the hyperpolarized compound of interest.[22] Transition-metal particles based on Pt, Pd, and Rh have been previously reported as capable heterogeneous catalysts for PHIP with a variety of substrate molecules, but none have been used for in vivo imaging because of the reduced polarization values.[23–25]

[*] J. McCormick, Dr. Y. N. Ertas, Z. Liu, L. Verlinsky, Prof. L.-S. Bouchard
Department of Chemistry and Biochemistry
University of California at Los Angeles
607 Charles E Young Drive East, Los Angeles, CA 90095-1569 (USA)
E-mail: louis.bouchard@gmail.com
Dr. S. Korchak, Dr. S. Mamone, Dr. S. Glöggler
Research Group for NMR Signal Enhancement
Max Planck Institute for Biophysical Chemistry
Am Fassberg 11, 37077 Göttingen (Germany)
and
Center for Biostructural Imaging of Neurodegeneration
Von-Siebold-Str. 3A, 37075 Göttingen (Germany)
E-mail: stefan.gloeggler@mpibpc.mpg.de
Dr. Y. N. Ertas, Prof. L.-S. Bouchard
Department of Bioengineering
University of California at Los Angeles
607 Charles E Young Drive East, Los Angeles, CA 90095-1569 (USA)
Dr. S. Wagner
Biomedical Imaging Research Institute, Cedars-Sinai Medical Center
8700 Beverly Blvd, Davis Building G149E
Los Angeles, CA 90048 (USA)
Prof. L.-S. Bouchard
The Molecular Biology Institute, Jonsson Comprehensive Cancer Center, California NanoSystems Institute
University of California at Los Angeles (USA)
Supporting information and the ORCID identification number(s) for the author(s) of this article can be found under: https://doi.org/10.1002/anie.201804185.

Herein, we introduce an N-acetylcysteine (NAC) stabilized metal catalyst using rhodium (Rh) to produce the new heterogeneous nanoparticle, NAC@Rh. This catalyst allows for efficient polarization of quaternary ^{15}N nuclei with long relaxation times. NAC-stabilized metal nanoparticles have recently been demonstrated to generate ^{1}H polarizations exceeding 1% in water;[26] these polarizations are measured values without compensation for signal decay loss from transit to the spectrometer. Since ^{1}H polarization decays within seconds owing to short longitudinal spin relaxation times T_1, the preservation of polarization by transfer to nearby nuclei such as ^{13}C, which have a T_1 on the order of a minute, or ^{15}N, which can have T_1 on the order of tens of minutes, is essential for clinical utilization.[27] Because of the very long relaxation time of ^{15}N, it could have a distinct advantage over for ^{13}C for clinical applications. Thus, the hyperpolarization of ^{15}N nuclei in contrast agents is of high interest. Since the gyromagnetic ratios (γ) of ^{15}N and ^{13}C are substantially lower than ^{1}H, imaging resolution will be inherently lower with comparable gradients, but strategies to overcome this by pulse transfer back to nearby ^{1}H before acquisition have been shown.[28]

While ^{13}C polarization levels exceeding 50% are readily achieved[1,29] in various injectable contrast agent systems in d-DNP, ^{15}N polarization levels obtained by d-DNP remain limited owing to the considerably lower gyromagnetic ratio γ of ^{15}N. Only recently, large ^{15}N polarization were achieved for the partially deuterated quaternary amine trimethylphenylammonium (TMPA) by cross-polarization DNP (CP-DNP).[30] The use of protonated compounds to achieve high polarization levels in CP-DNP typically results in ^{15}N relaxation times[22] shorter than in fully deuterated analogues. While 60–90% starting ^{1}H polarization was used for polarizing ^{15}N nuclei by cross-polarization, only $P_{15N} \approx 17\%$ was obtained after dissolution.[30]

To demonstrate the effectiveness of NAC@Rh in aqueous PHIP with respect to prior work, ^{13}C hyperpolarization in two compounds is investigated: the deuterated angiography contrast agent 1-^{13}C-hydroxyethyl propionate-d_3 (HEP)[31] and the metabolite derivative ethyl acetate (EA) upon hydrogenation of their respective precursors 1-^{13}C-hydroxyethyl acrylate-d_3 (HEA) and vinyl acetate (VA) with natural abundance ^{13}C. Enhancement of ^{13}C on HEP is observed upon transfer of nascent proton polarization to carbon by PH-INEPT+, a well-established polarization transfer pulse sequence for PHIP.[32] Polarization transfer from ^{1}H to ^{13}C after (para)-hydrogenation of VA into EA by field cycling between $B_0 \approx 50\ \mu T$ (Earth magnetic field) and $B_0 < 0.1\ \mu T$ inside a μ-metal chamber is also demonstrated. Unsaturated sidearm groups on acetate derivatives can be cleaved following polarization transfer to produce pure acetate,[33] a metabolite currently used in metabolic imaging.[34] To investigate hyperpolarization of ^{15}N, a nucleus found in many valuable metabolic probes, the deuterated precursor compound ^{15}N-neurine-d_{12} is available, producing d_{12}-^{15}N-ethyl trimethylammonium (NETMA) upon hydrogenation, a structural analogue of choline. Choline has previously been investigated as a metabolic probe by d-DNP[35] and positron emission tomography (PET)[36] owing to its role in the cellular phospholipid metabolism and has been used to probe upregulated choline kinase expression in malignant tissues[37] and other metabolic information.[38] However, production of hyperpolarized choline from the precursor substrate has not been demonstrated, most likely because the tautomerization between the keto and enol state prevents adequate hydrogenation.

After significant ^{1}H polarization was observed following neurine hydrogenation with NAC@Rh ($5.4 \pm 0.6\%$), a recently demonstrated heteronuclear transfer sequence, titled ESOTHERIC,[39] was employed for polarization transfer to ^{15}N. This sequence is well-suited for NETMA as it is able to transfer the nascent para-H_2 longitudinal two-spin order into observable in-phase heteronuclear magnetization in weakly coupled spin systems.[39] This is the first reported method for achieving high ^{15}N hyperpolarization by pulse transfer with aqueous PHIP.[40] The relevant precursors and products used in this work as well as the relevant J-couplings are shown in Figure 1.

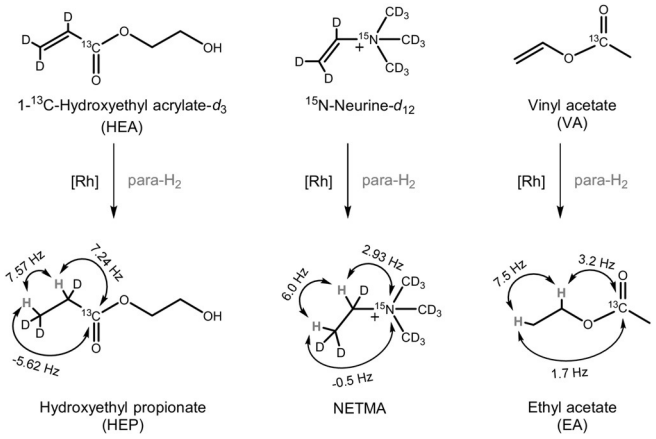

Figure 1. Reaction mechanisms of HEA, neurine, and VA hydrogenation. J_{AA}, J_{AX}, and $J_{A'X}$ values are considered in polarization transfer strategy from ^{1}H to ^{13}C and ^{15}N.

An essential component to advancing PHIP methodologies for in vivo applications is the ability to store nascent polarization as long-lived heteronuclear longitudinal magnetization to allow detection of the enhanced signal after delivery to the target tissues. Unlike previous homogeneous catalysts, namely Rh[1,4-bis(diphenylphosphino)butane](norbornadiene)BF_4 and its derivatives,[10,33,41,42] heterogeneous hydrogenations occurring on a metal surface can lead to randomization of the hydrogen spins. Ligand design not only allows dispersion and particle size control but favors pairwise para-H_2 addition by restricting hydride diffusion during hydrogenation, thus preserving the spin order of para-H_2 and hence observable polarization. Cysteine derivatives provide convenient thiol and amine groups which coordinate strongly to transition metals and form stable colloids, as well as suspension in water. Rh has been used in traditionally homogeneous PHIP catalysis and recently in heterogeneous catalysts (HET-PHIP),[22,23] where it has been shown to produce higher polarization than Ir, Pt, and Pd systems in similar immobilized materials.[43]

PHIP spectra for all compounds investigated are shown in Figure 2 and polarization levels are summarized in Table 1. The polarization method used for each compound was match to the methods available to us that has been used in past reports[26] and the scalar coupling[33] to achieve detectable polarization. Following application of the ESOTHERIC pulse, $P_{^{15}N}$ of 12.2 ± 2.7 % shown in Figure 2c and d was observed with NETMA, representing a 12.5-fold improvement over the highest previously recorded ^{15}N PHIP polarization of ^{15}N-propargylcholine using a homogeneous catalyst,[44] and a 186-fold improvement over previous aqueous HET-PHIP values.[22] Transfer to ^{13}C on HEP by PH-INEPT+ and EA by field cycling yielded $P_{^{13}C}$ of 3.2 ± 0.3 % and 1.3 ± 0.3 % respectively, representing 2.67-fold and 6.5-fold improvements over previous aqueous HET-PHIP investigations.[26] Thus the NAC@Rh effectiveness is not exclusive to ^{15}N and demonstrates a greater overall utility than previous metal nanoparticle catalysts across PHIP polarization methods.

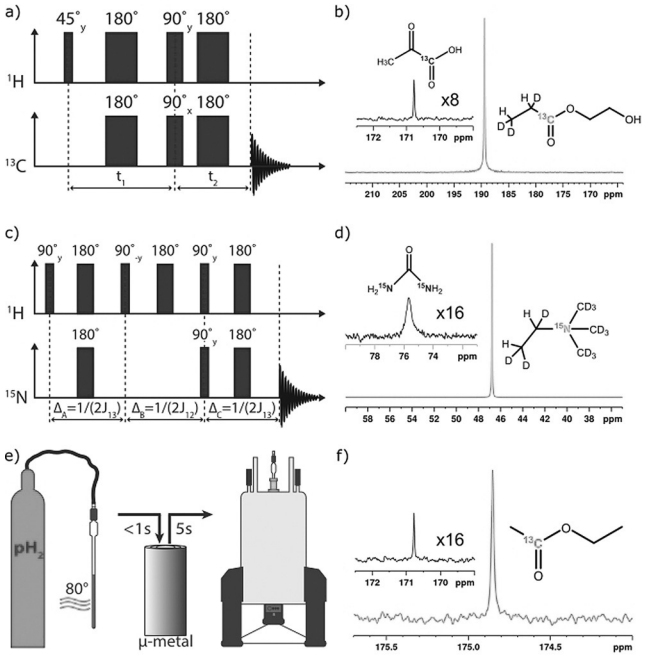

Figure 2. Pulse diagram for a) PH-INEPT+ applied to HEP with t_1 = 69.8 ms and t_2 = 38.9 ms in agreement with previous work[45] and b) Single ^{13}C scan of HEP following pulse (gray) and single 90° scan of reference 100 mM ^{13}C pyruvate solution (black) with vertical scaling. c) ESOTHERIC pulse using timings $\Delta_A = \Delta_C$ = 172.4 ms and Δ_B = 83 ms corresponding to couplings $J_{AA'}$ = 6.0 Hz, J_{AX} = −0.5 Hz, and $J_{A'X}$ = 2.93 Hz applied to NETMA following hydrogenation and d) Single ^{15}N scan of NETMA following application of ESOTHERIC pulse sequence (gray) and single reference 90° scan of 2 M ^{15}N-urea solution (black) with vertical scaling. e) Representation of field cycling transport out of zero field over 5 s following EA hydrogenation at Earth field consistent with previous reports[26,33] before insertion into the magnet and f) single 90° ^{13}C scan of EA following transport out of zero field (gray) and inlet thermal spectrum after 512 scans (black) with vertical scaling. Natural abundance vinyl acetate was used (^{13}C, 1.1 %). All experiments performed with 1 mM precursor concentration.

Table 1: Product properties and enhancements with NAC@Rh measured at 7 T.

Method	NETMA ESOTHERIC	HEP PH-INEPT+	EA Zero Field
^{1}H T_1 [s]	11.7 ± 1.2, 22.5 ± 2.4	4.0 ± 0.5	5.0 ± 0.7
^{1}H P%	5.4 ± 0.6	3.2 ± 0.3	2.1 ± 0.3[a]
^{13}C/^{15}N T_1 [s]	1259 ± 22[a]	55.6 ± 5.6	65.2 ± 0.4
^{13}C/^{15}N P%	12.2 ± 2.7	3.2 ± 0.2	1.3 ± 0.2[a]
TOF [h^{-1}]	44.9	71.8	51.3

[a] Measured at 14.1 T.

These results also highlight a key advantage for HET-PHIP, which is the stability of metal surfaces used for PHIP of nitrogenous compounds. Because nitrogen groups are excellent electron donors to transition metals, homogeneous catalysts often undergo rapid degradation as alkenes are out-competed by nitrogen groups forming inactive complexes. Upon investigation of NETMA formation using 5 mM homogeneous Rh[1,4-Bis(diphenylphosphino]butane)(cyclooctadiene)BF_4 catalyst, less than 1 % ^{1}H polarization is observed along with discolored precipitate forming in reaction tubes. Despite generally higher turnover frequency (TOF), a measurement of hydrogenation rate, homogeneous complexes are unable to polarize ^{15}N efficiently, as is evidenced by unprecedented ^{1}H polarization of an unprotected amino acid recently reported with a heterogeneous catalyst.[26]

The ^{15}N environment of NETMA is particularly well-suited for storing polarization in the form of longitudinal magnetization. The deuteration of the NETMA product contributes to long methyl and methylene ^{1}H T_1 times (11.7 s and 22.5 s, respectively), as shown in Table 1. This allows long ^{1}H polarization buildup times during para-H_2 bubbling before polarization transfer as well as particularly long ^{15}N T_1 relaxation times. A previous ^{15}N PHIP investigation of NETMA assessed the ^{15}N T_1 at 493 s (field strength of 9.4 T) by fitting the data to polarization decay without compensation for the 10° sampling pulses.[22] Investigation shown in Figure 3 by inversion recovery reveals a T_1 of 1259 ± 22 s (21.0 ± 0.4 min) under inert conditions and only a slight drop to 1003 ± 10 s (16.7 ± 0.2 min) under air atmosphere at 14 T. This allows a system where large ^{15}N polarization is generated, then separated from the catalyst and injected while

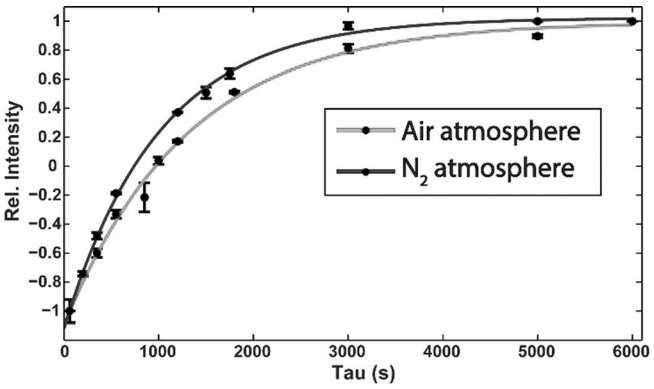

Figure 3. Inversion recovery plot of NETMA ^{15}N in D_2O yielding a) 21.0 ± 0.4 min and b) 16.7 ± 0.2 min longitudinal relaxation (T_1) under inert (N_2) and air atmospheres, respectively.

still retaining over 50% of its original intensity after 14 min, a substantial benefit for medical translation.

High polarization levels on ^{15}N were obtained by using the ESOTHERIC pulse sequence which is suited for transferring the nascent ^{1}H polarization to a heteronucleus in systems where the added proton pair is 1) weakly coupled and 2) asymmetrically coupled to the heteronucleus. Since this applies in NETMA, ESOTHERIC can theoretically transfer close to 95% spin order transfer (SOT) from two spin longitudinal order of protons after (para)-hydrogenation to the target nucleus (^{15}N). A more detailed explanation of the polarization transfer mechanism can be found elsewhere.[39] In traditional PASADENA experiments at high field, initially a 45° pulse is applied to detect the ^{1}H signal, achieving a theoretical maximum of 50% SOT, as investigated elsewhere.[45] After a 45° pulse was used to detect the ^{1}H signal, $P_{^{1}H} = 5.4 \pm 0.6\%$ was observed here in NETMA, this is thus half the spin–order polarization. Application of the ESOTHERIC sequence yields $P_{^{15}N} = 12.2 \pm 2.7\%$, showing that within the error, nearly unitary SOT is achievable as observable heteronuclear polarization. To our knowledge, this represents the most efficient ^{15}N transfer obtained with PHIP at high field.

Table 1 also outlines TOF rates for each contrast agent investigated. Dispersible colloid catalysts tend to suffer activity loss owing to surface coverage of ligand in place of potential catalytic sites, typically yielding a much lower TOF than heterogeneous catalysts capable of robust polarization. TOF for HEP using NAC@Rh shows 1.67-fold and 3.31-fold improvement over previous NAC@Pd and LCys@Pd catalyst systems, respectively under identical experimental conditions. This represents the ability to generate 5.52 mM of HEP in the 15 s required to hydrogenate using a small para-H_2 volume in an NMR tube and apply transfer polarization methodologies. Future work at higher generated product concentrations is still needed.

Heterogeneous catalysts in water are highly sought in PHIP experiments because they enable separation of the nascent hyperpolarized products, eliminating toxicity concerns regarding the injection of harmful materials into human patients.[23] Unprecedented ^{15}N polarization of NETMA in water along with benchmark ^{13}C enhancements on HEP and EA demonstrates NAC@Rh as a promising catalytic system for aqueous PHIP. This work is the first step in making in vivo PHIP[17–21] accessible for human use. As surface ligand interactions are better optimized, achievable polarizations of slow-relaxing nuclei such as ^{13}C and ^{15}N increase as well. These stabilized metal catalytic systems are conducive to catalyst removal and clean biocompatible product solutions ready for injection.

Acknowledgements

The authors acknowledge support from the National Science Foundation (NSF) (research grants CHE-1153159, CHE-1508707, equipment grant CHE-1048804), the Arnold and Mabel Beckman Foundation, the Jonsson Comprehensive Cancer Center Foundation at UCLA, the Max Planck Institute for Biophysical Chemistry, and the Stefan Hell Research Fellowship for mitigating collaboration on this work. We also acknowledge the use of ICP-MS facility within the UC Center for Environmental Implications of Nanotechnology in CNSI at UCLA.

Conflict of interest

The authors declare no conflict of interest.

Keywords: heterogeneous catalysis · hyperpolarization · parahydrogen-induced polarization · polarization transfer · rhodium nanoparticles

How to cite: *Angew. Chem. Int. Ed.* **2018**, *57*, 10692–10696
Angew. Chem. **2018**, *130*, 10852–10856

[1] S. J. Nelson, J. Kurhanewicz, D. B. Vigneron, P. E. Z. Larson, A. L. Harzstark, M. Ferrone, M. van Criekinge, J. W. Chang, R. Bok, I. Park, et al., *Sci. Transl. Med.* **2013**, *5*, 198ra108.
[2] C. H. Cunningham, J. Y. C. Lau, A. P. Chen, B. J. Geraghty, W. J. Perks, I. Roifman, G. A. Wright, K. A. Connelly, *Circ. Res.* **2016**, *119*, 1177–1182.
[3] T. H. Witney, M. I. Kettunen, D. E. Hu, F. A. Gallagher, S. E. Bohndiek, R. Napolitano, K. M. Brindle, *Br. J. Cancer* **2010**, *103*, 1400–1406.
[4] K. Golman, J. H. Ardenkjaer-Larsen, J. S. Petersson, S. Mansson, I. Leunbach, *Proc. Natl. Acad. Sci. USA* **2003**, *100*, 10435–10439.
[5] J. H. Ardenkjaer-Larsen, B. Fridlund, A. Gram, G. Hansson, L. Hansson, M. H. Lerche, R. Servin, M. Thaning, K. Golman, *Proc. Natl. Acad. Sci. USA* **2003**, *100*, 10158–10163.
[6] C. R. Bowers, D. P. Weitekamp, *J. Am. Chem. Soc.* **1987**, *109*, 5541–5542.
[7] J. Hovener, A. N. Pravdivtsev, B. Kidd, C. R. Bowers, S. Glöggler, K. V. Kovtunov, M. Plaumann, R. Katz-Brull, K. Buckenmaier, A. Jerschow, et al., *Angew. Chem. Int. Ed.* **2018**, *57*, 1034–1038; *Angew. Chem.* **2018**, *130*, 1046–1050.
[8] T. C. Eisenschmid, R. U. Kirss, P. P. Deutsch, S. I. Hommeltoft, R. Eisenberg, J. Bargon, R. G. Lawler, A. L. Balch, *J. Am. Chem. Soc.* **1987**, *109*, 8089–8091.
[9] R. W. Adams, J. A. Aguilar, K. D. Atkinson, M. J. Cowley, P. I. P. Elliott, S. B. Duckett, G. G. R. Green, I. G. Khazal, J. López-Serrano, D. C. Williamson, *Science* **2009**, *323*, 1708–1711.
[10] R. V. Shchepin, A. M. Coffey, K. W. Waddell, E. Y. Chekmenev, *J. Phys. Chem. Lett.* **2012**, *3*, 3281–3285.
[11] E. Cavallari, C. Carrera, S. Aime, F. Reineri, *J. Magn. Reson.* **2018**, *289*, 12–17.
[12] J. F. P. Colell, M. Emondts, A. W. J. Logan, K. Shen, J. Bae, R. V. Shchepin, G. X. Ortiz, P. Spannring, Q. Wang, S. J. Malcolmson, et al., *J. Am. Chem. Soc.* **2017**, *139*, 7761–7767.
[13] D. A. Barskiy, R. V. Shchepin, A. M. Coffey, T. Theis, W. S. Warren, B. M. Goodson, E. Y. Chekmenev, *J. Am. Chem. Soc.* **2016**, *138*, 8080–8083.
[14] R. V. Shchepin, D. A. Barskiy, A. M. Coffey, T. Theis, F. Shi, W. S. Warren, B. M. Goodson, E. Y. Chekmenev, *ACS Sens.* **2016**, *1*, 640–644.
[15] F. Shi, A. M. Coffey, K. W. Waddell, E. Y. Chekmenev, B. M. Goodson, *Angew. Chem. Int. Ed.* **2014**, *53*, 7495–7498; *Angew. Chem.* **2014**, *126*, 7625–7628.
[16] K. V. Kovtunov, L. M. Kovtunova, M. E. Gemeinhardt, A. V. Bukhtiyarov, J. Gesiorski, V. I. Bukhtiyarov, E. Y. Chekmenev, I. V. Koptyug, B. M. Goodson, *Angew. Chem. Int. Ed.* **2017**, *56*, 10433–10437; *Angew. Chem.* **2017**, *129*, 10569–10573.

[17] A. M. Coffey, R. V. Shchepin, M. L. Truong, K. Wilkens, W. Pham, E. Y. Chekmenev, *Anal. Chem.* **2016**, *88*, 8279 – 8288.
[18] P. Bhattacharya, K. Harris, A. P. Lin, M. Mansson, V. A. Norton, W. H. Perman, D. P. Weitekamp, B. D. Ross, *Magn. Reson. Mater. Phys. Biol. Med.* **2005**, *18*, 245 – 256.
[19] P. Bhattacharya, E. Y. Chekmenev, W. F. Reynolds, S. Wagner, N. Zacharias, H. R. Chan, R. Bünger, B. D. Ross, *NMR Biomed.* **2011**, *24*, 1023 – 1028.
[20] M. Ishii, K. Emami, S. Kadlecek, J. S. Petersson, K. Golman, V. Vahdat, J. Yu, R. V. Cadman, J. MacDuffie-Woodburn, M. Stephen, et al., *Magn. Reson. Med.* **2007**, *57*, 459 – 463.
[21] M. Goldman, H. Jóhannesson, O. Axelsson, M. Karlsson, *Magn. Reson. Imaging* **2005**, *23*, 153 – 157.
[22] L. B. Bales, K. V. Kovtunov, D. A. Barskiy, R. V. Shchepin, A. M. Coffey, L. M. Kovtunova, A. V. Bukhtiyarov, M. A. Feldman, V. I. Bukhtiyarov, E. Y. Chekmenev, et al., *J. Phys. Chem. C* **2017**, *121*, 15304 – 15309.
[23] K. V. Kovtunov, D. A. Barskiy, R. V. Shchepin, O. G. Salnikov, I. P. Prosvirin, A. V. Bukhtiyarov, L. M. Kovtunova, V. I. Bukhtiyarov, I. V. Koptyug, E. Y. Chekmenev, *Chem. Eur. J.* **2016**, *22*, 16446 – 16449.
[24] S. Glöggler, A. M. Grunfeld, Y. N. Ertas, J. McCormick, S. Wagner, P. P. M. Schleker, L. S. Bouchard, *Angew. Chem. Int. Ed.* **2015**, *54*, 2452 – 2456; *Angew. Chem.* **2015**, *127*, 2482 – 2486.
[25] E. W. Zhao, R. Maligal-Ganesh, C. Xiao, T. W. Goh, Z. Qi, Y. Pei, H. E. Hagelin-Weaver, W. Huang, C. R. Bowers, *Angew. Chem. Int. Ed.* **2017**, *56*, 3925 – 3929; *Angew. Chem.* **2017**, *129*, 3983 – 3987.
[26] J. McCormick, A. M. Grunfeld, Y. N. Ertas, A. N. Biswas, K. L. Marsh, S. Wagner, S. Glöggler, L. S. Bouchard, *Anal. Chem.* **2017**, *89*, 7190 – 7194.
[27] H. Nonaka, R. Hata, T. Doura, T. Nishihara, K. Kumagai, M. Akakabe, M. Tsuda, K. Ichikawa, S. Sando, *Nat. Commun.* **2013**, https://doi.org/10.1038/ncomms3411.
[28] C. von Morze, G. D. Reed, P. E. Larson, D. Mammoli, A. P. Chen, J. Tropp, M. Van Criekinge, M. A. Ohliger, J. Kurhanewicz, D. B. Vigneron, et al., *Magn. Reson. Med.* **2018**, *80*, 480 – 487.
[29] H. A. I. Yoshihara, E. Can, M. Karlsson, M. H. Lerche, J. Schwitter, A. Comment, *Phys. Chem. Chem. Phys.* **2016**, *18*, 12409 – 12413.
[30] J. Milani, B. Vuichoud, A. Bornet, R. Melzi, S. Jannin, G. Bodenhausen, *Rev. Sci. Instrum.* **2017**, https://doi.org/10.1063/1.4973777.
[31] K. Golman, O. Axelsson, H. Jóhannesson, S. Månsson, C. Olofsson, J. S. Petersson, *Magn. Reson. Med.* **2001**, *46*, 1 – 5.
[32] M. Haake, J. Natterer, J. Bargon, *J. Am. Chem. Soc.* **1996**, *118*, 8688 – 8691.
[33] F. Reineri, T. Boi, S. Aime, *Nat. Commun.* **2015**, *6*, 5858.
[34] A. Flori, M. Liserani, F. Frijia, G. Giovannetti, V. Lionetti, V. Casieri, V. Positano, G. D. Aquaro, F. A. Recchia, M. F. Santarelli, et al., *Contrast Media Mol. Imaging* **2015**, *10*, 194 – 202.
[35] C. Gabellieri, S. Reynolds, A. Lavie, G. S. Payne, M. O. Leach, T. R. Eykyn, *J. Am. Chem. Soc.* **2008**, *130*, 4598 – 4599.
[36] I. J. De Jong, J. Pruim, P. H. Elsinga, W. Vaalburg, H. J. A. Mensink, G. Jakse, *Eur. Urol.* **2003**, *44*, 32 – 39.
[37] G. Eliyahu, T. Kreizman, H. Degani, *Int. J. Cancer* **2007**, *120*, 1721 – 1730.
[38] F. Podo, S. Canevari, R. Canese, M. E. Pisanu, A. Ricci, E. Iorio, *Exp. Oncol.* **2011**, *19*, 1 – 10.
[39] S. Korchak, S. Yang, S. Mamone, S. Glöggler, *ChemistryOpen* **2018**, *7*, 344 – 348.
[40] T. Theis, M. Truong, A. M. Coffey, E. Y. Chekmenev, W. S. Warren, *J. Magn. Reson.* **2014**, *248*, 23 – 26.
[41] R. V. Shchepin, A. M. Coffey, K. W. Waddell, E. Y. Chekmenev, *Anal. Chem.* **2014**, *86*, 5601 – 5605.
[42] P. Hübler, R. Giernoth, G. Kümmerle, J. Bargon, *J. Am. Chem. Soc.* **1999**, *121*, 5311 – 5318.
[43] U. Obenaus, S. Lang, R. Himmelmann, M. Hunger, *J. Phys. Chem. C* **2017**, *121*, 9953 – 9962.
[44] F. Reineri, A. Viale, S. Ellena, D. Alberti, T. Boi, G. B. Giovenzana, R. Gobetto, S. S. D. Premkumar, S. Aime, *J. Am. Chem. Soc.* **2012**, *134*, 11146 – 11152.
[45] A. B. Schmidt, S. Berner, W. Schimpf, C. Müller, T. Lickert, N. Schwaderlapp, S. Knecht, J. G. Skinner, A. Dost, P. Rovedo, et al., *Nat. Commun.* **2017**, https://doi.org/10.1038/ncomms14535.

Manuscript received: April 9, 2018
Revised manuscript received: June 14, 2018
Accepted manuscript online: June 19, 2018
Version of record online: July 9, 2018

